Toward a Wireless Optical Communication Link between Two Small Unmanned Aerial Vehicles

M. Last, B.S. Leibowitz, B. Cagdaser, A. Jog, L. Zhou, B. Boser, K.S.J. Pister

Berkeley Sensor and Actuator Center
497 Cory Hall, UC Berkeley
Berkeley, CA 94720-1774, USA

ABSTRACT

A communication system between two autonomous micro air vehicles is proposed. Laser communication offers advantages in range, power, and bandwidth when line of sight is available. Beamsteering is accomplished using gyro-stabilized MEMS micromirrors. A custom CMOS smart-pixel imager implements a 1Mbps receiver, including analog front-end and variable-gain amplifier at each pixel. Algorithms are presented for initial link establishment and maintenance.

1. INTRODUCTION

This paper describes our efforts to date to build a multi-kilometer megabit per second free-space wireless optical link between two micro air vehicles.

For applications where line-of-sight is guaranteed, optical wireless communication offers significant advantages over radio frequency (RF) communication due to the highly collimated beams that can be generated. These tightly focused beams are made possible by the short wavelengths of visible light, and can be thought of as an enormous antenna gain that can be used to decrease the transmitted power, increase the communication range, and increase the bandwidth compared to an RF link. In addition, the highly directional nature of a laser link makes eavesdropping difficult.

The downside of using such a highly directional link is the need to keep the laser aligned with the intended receiver. This is made even more difficult when the transmitting platform is in motion. In power- and weight-constrained situations, such as micro-air-vehicle to micro-air-vehicle applications, no technologies are available that can keep a laser beam on-target given the dynamics of the micro-air-vehicle.

Using inertial measurement devices and beamsteering optics based on micro-electromechanical systems (MEMS) tightly coupled with CMOS smart-pixel imaging arrays, we are building a novel free-space optical communication system optimized for space, weight, and power consumption.

In this paper, we provide an overview of the system constraints and show how we will build and integrate components that will meet these constraints. Section 2 presents the constraints imposed by the micro-air-vehicle that we are using as our mobile platform. Section 3 talks about the hardware we are building that implement our beamsteering transmitter and optical receiver. In section 4, we discuss the algorithms used to initiate and maintain the alignment of the bidirectional laser communication link. Finally, we summarize the paper and talk about future work.

2. SYSTEM CONSTRAINTS

2.1 Micro Air Vehicle

Two 1.5m wingspan MLB Bats[1] serve as the aerial platform for our communication system. Each Bat has a custom pod mounted on it that serves as the housing for our equipment. Since the Bat can accept a maximum payload of 2 lbs (including the weight of the pod itself), the weight of all components must be minimized. Sensor-actuator alignment, weight, and space considerations serve as the primary design constraints. Eye safety limits our average laser output power to 5mW.

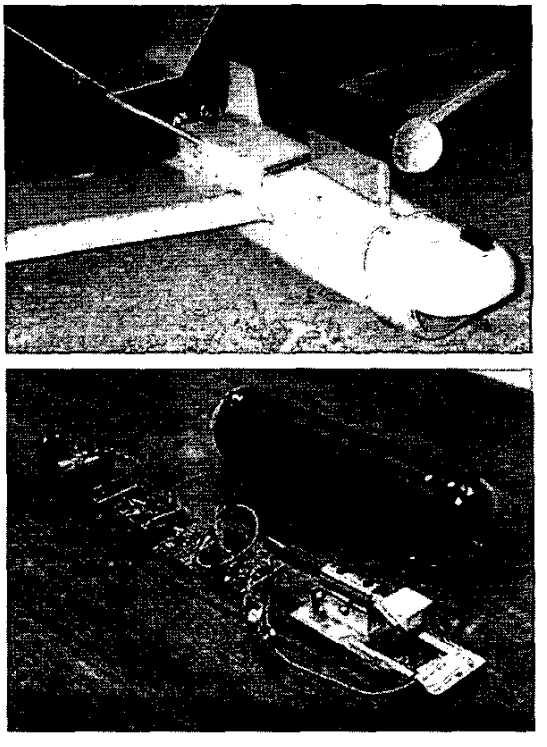

Figure 1: Pod mounted on MLB Bat (Top). Functional prototype of battery-powered gyro-stabilized MEMS scanner (Bottom).

Angular vibrations present on each airplane can be as large as +/- 5 deg optical, which can be cancelled by +/- 2.5° mechanical rotation of the mirror. In addition to these vibrations, the angle to the second plane is not known precisely (imagine the airplane in a strong

0-7803-7761-3/03/$17.00 ©2003 IEEE

crosswind – the direction the airplane is going is not the direction the airplane is pointing). An extra +/-7.5° margin is provided in the design of the beamsteering mirror to accommodate this error. The bandwidth of the airplane dynamics consists of low-frequency modes in the sub-10Hz range, and extends out past 300Hz. The low-frequency oscillations are caused by lightly damped aerodynamic modes and flight maneuvers. The high frequency modes are due to engine vibration. With suitable isolation mounts, the high-frequency

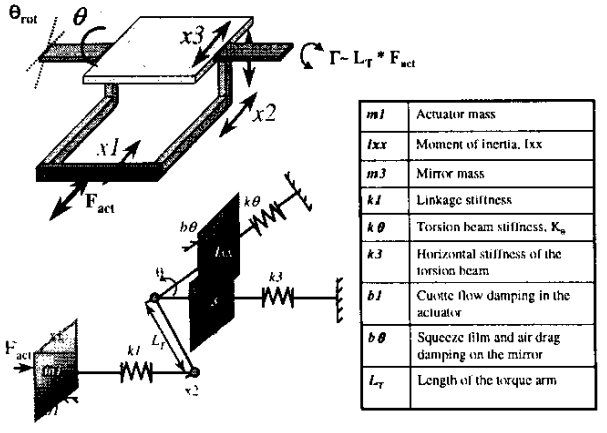

m1	Actuator mass
Ixx	Moment of inertia, Ixx
m3	Mirror mass
k1	Linkage stiffness
kθ	Torsion beam stiffness, K_θ
k3	Horizontal stiffness of the torsion beam
b1	Couette flow damping in the actuator
bθ	Squeeze film and air drag damping on the mirror
L_T	Length of the torque arm

Figure 2: Analytical model of a 1 DOF mirror.

noise can be filtered. However, the low-frequency noise caused by rigid-body movement of the aircraft must be measured and compensated for. These aircraft dynamics, especially rotations, require the use of feedforward control using MEMS gyroscopes in order to maintain the link for more than a fraction of a second.

A landing shock of approximately 10-15g is easily isolated by appropriate mounting hardware. A takeoff shock during the catapult launch is estimated to be only about 5g. The MEMS mirrors are designed to accept shocks well in excess of 200g.

3. HARDWARE

3.1 Beamsteering Transmitter

The beam used for the transmission has a diffraction-limited full-width-half-max (FWHM) beam width of 1 mrad (.057 deg), providing the necessary antenna gain for reception of the signal (see section 3.2). This diffraction limited aperture is defined by the size of a MEMS two-axis beam steering mirror. Considering the need for an uninterrupted illumination at the receiver end, error margin for pointing imperfections becomes a small fraction of 1 mrad, which sets the specs for pointing accuracy. Motion of the two ends and the host vehicle vibration require a tracking and pointing stabilization system. Previous work showed that periodic dithering can provide the beam heading with slow updates, which achieves tracking and keeps the drift of beam heading bounded[2].

Taking into account the needs for acquisition and vibration canceling, the range of bi-directional steering needed for our application is approximately +/-5° mechanical about both azimuth and elevation axes. Considering the 1mrad FWHM beam, the system needs an actuator with more than 60 dB dynamic range. Nonlinear characteristics of torsion beams, dependence on ambient conditions, and possible hysteresis in the actuator are important obstacles for achieving the needed resolution by using open loop control. Besides these obstacles, the MEMS mirrors we have built[3,4,5] are high Q systems and prone to ringing when actuated by wide band signals. Squeeze film damping, the major damping source, is not sufficient due to the absence of substrate underneath the mirror body. Experimental results showed longer than 10 ms significant ringing, which is intolerable for system requirements.

The proposed solution for achieving actuation goals is implementing a closed loop position feedback control. Implementation of the loop requires a detailed model of the mirror. In addition to that we need to implement a sensor for reading the current position of the mirror.

Attaching sense fingers to the actuators is the most efficient way to perform position sensing without greatly affecting the mirror dynamics. Additionally, sensing and driving from the same place provides benefits when designing a control system.

In our modeling work, we took three main dynamics into account. These three dynamics are rotation, lateral motion of the mirror along the direction that actuator is pushing/pulling, and the linkage compliance. We considered these to be important in the sense that they directly affect the actuation motion as detected by the sense fingers. We used FEA simulations performed using ANSYS for verifying analytical models. Figure 2 shows a detailed mass-spring-damper equivalent system of a 1 DOF mirror. The model shown takes only the above mentioned three dynamics into account. Other dynamics, such as the flexing of the mirror under angular acceleration, are not modeled and therefore will not be controlled.

3.2 Optical Receiver

Optical detection is accomplished with a fully integrated CMOS "smart pixel" receiver. The diffraction limit for the peak on axis optical intensity with a 1 mm transmission aperture and a 680 nm, 5 mW average power laser is 670 $\mu W/m^2$ at a range of 5 km (neglecting tubulence)[6]. Allowing for some loss in optical components, a 2 cm diameter receiver aperture could thus receive 75 nW (-41 dBm) of optical power at the half maximum diffraction angle of 0.5 mrad. With measured photodiode responsivity in excess of 0.2 A/W for the CMOS process in use, a 15 nA peak signal is generated at the receiver. The detection impedance and effective input transistor transconductance are thus chosen so that the input equivalent electronic noise will be less than 1 nA_{rms} with a 2 MHz bandwidth.

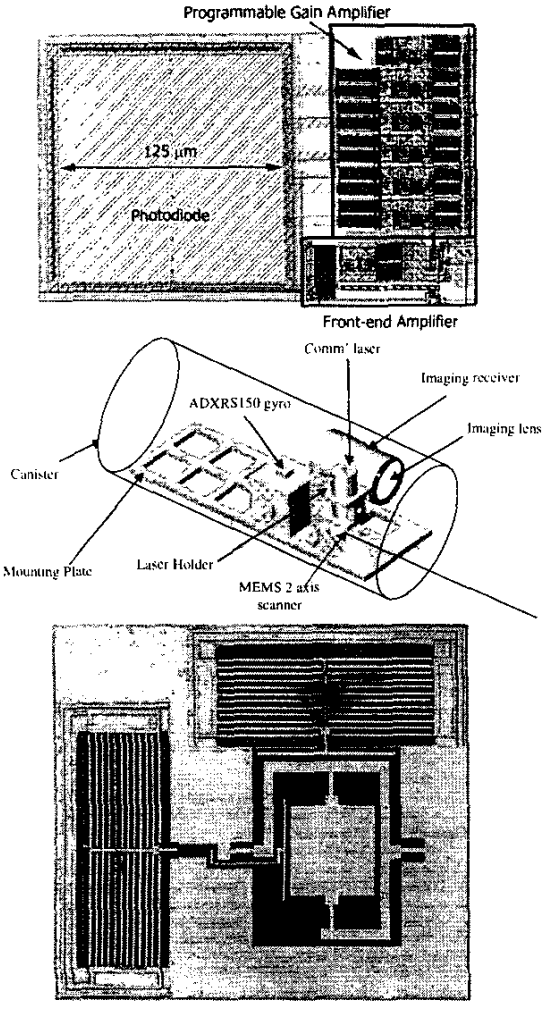

Figure 3: Schematic layout of next-generation pod transceiver (Center) integrating 2-axis MEMS pointing mirror (Bottom) and CMOS imaging receiver (layout of one pixel shown, Top). MEMS pointing mirror achieves 13°x6° optical deflection at 62.2V and 79.9V respectively.

However, with a 20 degree full field of view, shot noise due to ambient solar illumination (either direct from the sky or reflected from the ground) is a limiting factor even with the use of a 10 nm bandpass optical filter at the receiver. An imaging receiver can further decrease the effect of shot noise caused by ambient illumination. Such a receiver consists of an array of single channel optical receivers at the focal plane of an imaging lens, so that each receiver only detects the ambient light from a small portion of the field of view. But if the size of an individual receiver in the focal plane is much greater than the spot size of the imaging optic, then light collected from a particular transmission is likely to land entirely on one receiver element, resulting in an improvement of shot noise limited SNR by a factor equal to the array resolution. In this system the imaging receiver will consist of a 16×16 array of "smart pixels" fully integrated in a single die in a 0.25 µm foundry CMOS process. Each pixel will contain the necessary components for optical detection, amplification, signal processing, and logic to decode incoming serial data and communicate it via a common off-chip bus.

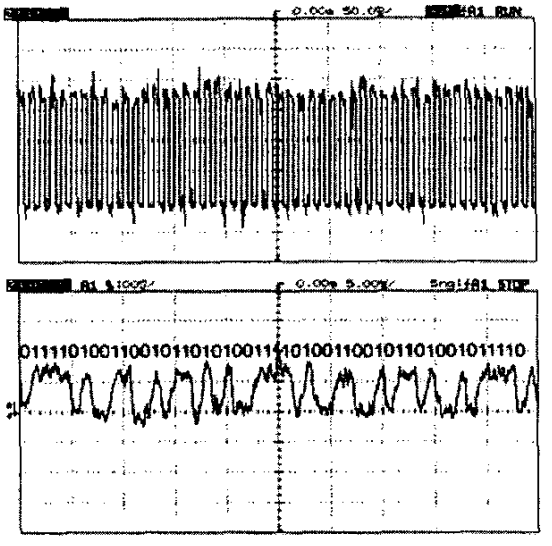

Figure 4: (Top) 100 Hz square wave transmission received over 250 m free-space link. Turbulent scintillation is approximately +/- 0.5 dB and on a msec or slower time scale. (Bottom) 1 Mbps transmission received over 5.1 km free-space link annotated with data. Turbulent scintillation led to low link availability at this range, but is clearly quasi-static at this time scale.

A single receiver pixel consisting of a photodiode, digitally programmable sense impedance, front-end amplifier, and digitally programmable variable gain amplifier (PGA) has been fabricated and tested both in a laboratory setting and in stationary free-space links at 250 m and 5.1 km ranges [Figure 4]. Due to this wide variation in link range, a very wide dynamic range is required. Sense impedance can varied from 1 kΩ to 100 kΩ in 20 dB steps. Gain can be programmed digitally over a 33 dB range in monotonic 3 dB steps, leading to an overall gain control range in excess of 70 dB. Gain control is designed to be fast enough to track turbulence induced scintillation in the received signal. However, the digital gain control loop is currently closed off-chip via a serial bus and is not fast enough for this task.

Under direct illumination in the laboratory this receiver has been demonstrated to detect signals as weak as 40 nW (-44 dBm) optical and over a 60 dB dynamic range (limited by peak power of available laser source). The active area of these components is approximately 125µm×200 µm. Stationary free space links at ranges of 250 m and 5.1 km were tested with a 2 cm diameter imaging lens and 15 mW average transmission power. These tests were performed at night to avoid the need for a narrow band pass optical filter. At 250 m the transmission was detected with 57 dB gain margin in the PGA and very little turbulent scintillation [Figure 4]. At 5.1 km a 1 Mbps transmissions was detected, but turbulent fading led to very low link availability [Figure 4]. Both links were performed at ground level and

in the presence of light haze, and across a body of water in the case of the 5.1 km link. Atmospheric turbulence is known to be less significant even at modest elevation from the ground, but modeling of this effect is still being researched.

3.3 System Integration

All system components are placed in a 3" diameter carbon fiber canister. Although aerodynamic considerations inhibit use of flat apertures, the hemispherical end caps are flattened in the regions in front of the imager and transmitter to reduce distortion.

We are developing a platform on which the three axis MEMS gyroscopes, the laser source, the MEMS 2-axis mirror system, and the smart pixel imaging receiver are mounted. The gyroscopes and the scanner misalignments must be calibrated. A die-package misalignment of +/- 1 degree is present in the gyroscopes while that in the scanner is not well controlled. Gyroscope misalignments translate into angular errors which over time results in link severance.

The mounting platform depicted schematically in Figure 3 has been built. Flexible circuit boards will be used to mount the MEMS scanner at a suitable tilt angle to ensure straight beam exit from the cannister at the mid-range of mirror excursion. An adjustable laser mount holds the modulatable 4.5mW light source. A hollow acrylic cube ensures gyroscope orthogonality within the limits of die-package misalignment. Three Analog Devices ADXRS150 yaw-rate MEMS gyroscopes are used for platform orientation detection. The 2 axis MEMS scanner is built in the UC Berkeley Microlab.

4. ALGORITHMS

4.1 Acquisition

The initial link setup is an iterative process. Planes A and B start by choosing the center of their field of view and scanning an expanding spiral pattern. The data packet each broadcasts at each point in the scan consists of a wakeup pulse train and the direction that it is pointing. Suppose A's laser hits B first. B will receive data in a given pixel of its imaging receiver, narrowing its search field to ~22mrad square. Centering its laser on the pixel, B initiates another spiral scan, broadcasting its direction and the direction A was pointing when it connected with B. When A receives the data B is transmitting, A swings its laser to the direction where B was able to receive data and initiates another spiral scan. The algorithm converges within one to two more spiral scan cycles and bidirectional communication is established.

Using this algorithm, there are two possible speed-limiting factors in acquisition: the dwell time at each direction required to send the data packet and the mirror speed. The dwell time requirement stems from the time required to set the gain controls in the receiver and the amount of data required to transmit the pointing angle. In this system, the speed limiting factor is the receiver, not the mirror.

4.2 Link Maintenance

Gyroscopes in the controller measure vibration. Since the measured signal is rotation rate, integration is necessary for an indirect angular measurement. The system subtracts measured disturbances from the steering angle in order to minimize the effects of platform jitter. The gyroscope output has inherent noise and drift on top of the desired rate signal. Integration causes accumulation of these errors in the beam heading. In addition to the noise related errors, the out-of-plane die-package misalignment of gyroscopes causes sensors to pick up signals cross- coupled from other axes, and add to the error in the vibration detection. The stabilization system cannot reject gyroscope originated errors due to the lack of having closed loop control of absolute beam orientation. The beam heading must be corrected with respect to an external reference. Dithering, which uses the receiver as a reference, is effective in canceling the errors accumulating in the beam heading.

Assuming the link between the two micro air vehicles is acquired, the position of the receiver relative to the center of the transmitted beam provides useful information for detecting the misalignment. The transmitting end periodically dithers the beam heading by amounts smaller than the beam width. Losing the link as a result of dithering indicates the direction of misalignment, and provides a rough estimation of its value. A correction following the detection keeps pointing errors bounded. Periodic application of the dithering method decreases the available data bandwidth and should therefore be done as infrequently as possible.

5. SUMMARY/GOALS

In this paper we present a steered laser communication system between two micro air vehicles designed to send data at megabit per second speeds. A MEMS beamsteering mirror and a custom CMOS smart pixel have been built.

Due to the extensive use of micromachined components and the high levels of integration possible with our approach, we project that we will integrate all of the main components, namely the beamsteering transmitter, imaging receiver, MEMS gyroscopes, custom CMOS signal processor, and passive components into a system that weighs under 30g, has less than a cubic inch displacement, and consumes less than 100mW.

---

[1] MLB Corporation, 137 Lundy Lane, Palo Alto, CA 94306. (650) 424-9552. http://www.spyplanes.com

[2] B. Cagdaser,B.Leibowitz, M. Last, K. Ramanathan, B.E. Boser, B. K.S.J. Pister, "Pointing error correction for MEMS laser communication sytems," *Proc. of the IASTED Intl. Conf. Automation, Control and Information Technology*, pp. 136-140, June 2002.

[3] Milanovic, Last, Pister, "Torsional Micromirrors with Lateral Actuators" *Transducers '01*, Muenchen, Germany, June 2001

[4] Milanovic, Last, Pister, "Laterally Actuated Torsional Micromirrors for Large Static Deflection" to appear in *IEEE Photonics Technology Letters*

[5] V. Milanovic, M. Last, K.S.J. Pister, "Monolithic Silicon Micromirrors with Large Scanning Angle," *Optical MEMS 2001*, Okinawa, Japan, Sep. 2001.

[6] Born, Wolf. Principles of Optics, 7th ed., pg. 440, Cambridge, UK: Cambridge University Press (1999).